

Long-term correction of GRAPES-3 muon telescope efficiency

P.K. Mohanty^{* a,b}, S. Ahmad^{a,g}, K.P. Arunbabu^{a,b}, A. Chandra^{a,b}, S.R. Dugad^{a,b}, S.K. Gupta^{a,b}, B. Hariharan^{a,b}, Y. Hayashi^{a,d}, P. Jagadeesan^{a,b}, A. Jain^{a,b}, V.B. Jhansi^{a,b}, S. Kawakami^{a,d}, H. Kojima^{a,e}, S.D. Morris^{a,b}, P.K. Nayak^{a,b}, A. Oshima^{a,f}, B.S. Rao^{a,b}, L.V. Reddy^{a,b}, S. Shibata^{a,f}, P. Subramanian^{a,c}, M. Zuberi^{a,b}

^aGRAPES-3 Experiment, Cosmic Ray Laboratory, Raj Bhavan, Ooty 643 001, India.

^bTata Institute of Fundamental Research, Homi Bhabha Road, Mumbai 400 005, India.

^cIndian Institute of Science Education and Research, Pune 411021, India

^dGraduate School of Science, Osaka City University, Osaka 558-8585, Japan

^eFaculty of Engineering, Aichi Institute of Technology, Toyota City, Aichi 470-0392, Japan

^fCollege of Engineering, Chubu University, Kasugai, Aichi 487-8501, Japan

^gAligarh Muslim University, Aligarh 202002, India

E-mail: pkm@tifr.res.in

The GRAPES-3 experiment in Ooty, India has been operating a large area (560 m²) tracking muon telescope since 2000. It consists of 16 identical modules and each one is designed to measure the flux of muons in 13 × 13 directions covering 2.3 sr field of view. The high statistics data has enabled to probe transient space weather events on time scale of minutes. Due to independent nature of operation of the modules, despite intermittent failure of individual modules, a continuity in rate could still be achieved. By correcting for transient instrumental problems and gradual efficiency variations, an uninterrupted muon record is being assembled which may prove to be a valuable database for probing both transient and long-term solar phenomena. Details of the efficiency correction technique will be presented during the conference.

35th International Cosmic Ray Conference — ICRC2017

10–20 July, 2017

Bexco, Busan, Korea

*Speaker.

1. Introduction

The GRAPES-3 is an extensive air shower (EAS) experiment, located in Ooty, India (11.4°N, 76.7°E and 2200 m altitude). It comprises of 400 plastic scintillator detectors of 1 m² area each, placed in 8 m separation [1] and a large area (560 m²) area tracking compact muon telescope [2]. The muon content in each EAS recorded exclusively by the muon telescope is used to extract the composition information of primary cosmic rays [3] and to discriminate γ -ray primaries against the huge background of charged cosmic rays [4].

The muon telescope comprises of 16 modules based on proportional counters (PRCs) of 6 m long and 10 cm \times 10 cm cross section steel tubes filled with P-10 gas (90% Ar + 10% CH₄) which serves as active detection medium. In each module, four layers of 58 PRCs in each were placed in a grid configuration to track and reconstruct the arrival direction of each muon from a varying zenith angle up to 60° covering a field of view of 2.3 sr [5]. Each module provides 35 m² area. Concrete of thickness 550 g cm⁻² has been placed above the PRC layers that allows penetrating muons of above 1 GeV to be recorded. The reconstructed muon directions are binned in 13 \times 13 (169). The muon telescope provides a two dimensional real-time monitor of the muon flux with an average angular resolution of 4°. Each module records $\sim 3 \times 10^3$ muons per second.

The GRAPES-3 muon telescope has been continuously operating since year 2000 and has recorded over 17 years of data that comprises more than 20 trillion muons. The unique combination of both high statistics and high angular resolution measurement has given GRAPES-3 unprecedented sensitivity to study both transient and long term space weather phenomena driven by coronal mass ejections (CMEs) [5, 6, 7, 8, 9, 10, 11]. However, the corrections of muon rates from the modulation of atmospheric pressure and temperature have to be made prior to any of the above studies. These effects have been precisely measured and corrected in the GRAPES-3 data [12, 13]. Further, the muon rates are significantly affected by long term efficiency variation of the modules in addition to short term fluctuations. Correction of these effects are necessary for reliable measurement of cosmic ray variation and the associated phenomena.

2. Muon module efficiency variation

Efficiency of each PRC determines the rate of a module. PRCs those are located at central region in the layer have more weight to the module rate. Most of the PRCs have been operating in a stable manner for many years together since their installation. However, minute leak occurring in a few PRC results gradual change in their efficiency. When a leak could be identified, the PRC is repaired and filled with P-10 gas. Despite of our best efforts, it couldn't have been possible to identify every minute leak. Therefore, employing software corrections of the efficiency variation is a viable option.

An example of an efficiency variation is shown in Fig. 1. The daily muon rate of the module 4 and 5 for a period of 100 days from 1 January to 10 April 2006 are shown in Fig. 1a and Fig. 1b. The similar profile of the rates observed in both modules are caused due to atmospheric and solar effects. The module 5 has exhibited relatively stable performance over a long period and therefore it has been chosen as the reference for the present study. By taking ratio of the rates of two modules, the atmospheric and pressure variations have been eliminated. The Fig. 1c have shown a systematically

decrease of 0.3% in the rate in module 4 relative to the module 5 in the 100 days period. Owing to the small statistical error ($\sim 0.01\%$) in the data, this systematic variation is significant to be considered.

3. Modeling efficiency variation

Efficiency variation of the modules were modeled by a fourth order polynomial as described below.

The rate of a module as a function of time 't' may be described as,

$$R(t) = R_0 \varepsilon(t) \quad (3.1)$$

Here $\varepsilon(t)$ represents the time varying part of the efficiency, approximated by a 4th order polynomial,

$$\varepsilon(t) = 1 + a_1 t + a_2 t^2 + a_3 t^3 + a_4 t^4 \quad (3.2)$$

The ratio of rates between two modules i, and j measured at time t_k is,

$$r_{ij}(t_k) = \frac{R_{0i}(1 + a_{1i}t_k + a_{2i}t_k^2 + a_{3i}t_k^3 + a_{4i}t_k^4)}{R_{0j}(1 + a_{1j}t_k + a_{2j}t_k^2 + a_{3j}t_k^3 + a_{4j}t_k^4)} \quad (3.3)$$

Assuming that the time dependent terms in $\varepsilon(t)$ are $\ll 1$, which is shown to be true later and taking the natural log of both sides in Eq. 3.3 followed by the use of approximation $\ln(1+x) \simeq x$, the resultant equation became linear in coefficients.

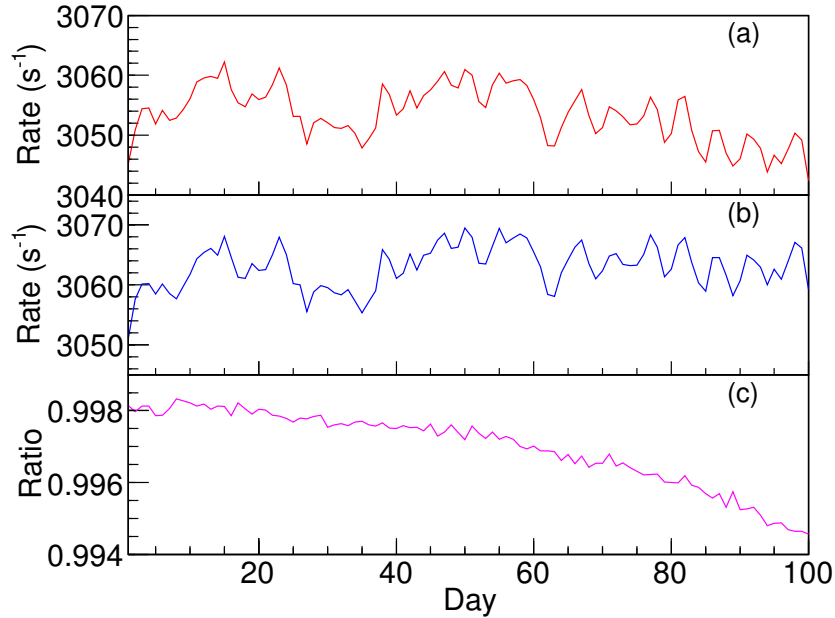


Figure 1: Variation in daily mean muon rate observed in (a) module 4, (b) module 5, and (c) ratio of 4 & 5 for 100 d (1 January – 10 April 2006).

$$\ln(r_{ij}(t_k)) = \ln(R_{0i}) - \ln(R_{0j}) + (a_{1i} - a_{1j})t_k + (a_{2i} - a_{2j})t_k^2 + (a_{3i} - a_{3j})t_k^3 + (a_{4i} - a_{4j})t_k^4 \quad (3.4)$$

redefining 'ln' terms, we obtained

$$f_{ij}(t_k) = a_{0i} - a_{0j} + (a_{1i} - a_{1j})t_k + (a_{2i} - a_{2j})t_k^2 + (a_{3i} - a_{3j})t_k^3 + (a_{4i} - a_{4j})t_k^4 \quad (3.5)$$

For 16 modules, there were ${}^{16}C_2 = 120$ independent ratios for each t_k value. While 'i' varied from 1 to 15, and 'j' from i+1 to 16 for incorporating every independent combination. For k ' t_k ' values, there are $120 \times k$ linear equations of the above form. The next task was to solve the set of linear equations simultaneously to obtain the 80 coefficients ('a' values) for the 16 modules with five 'a' values for each module. We represented the set of linear equations in a matrix form as shown below,

$$\sum_{l=0}^4 (a_{li} - a_{lj})t_k^l = f_{ij}(t_k) \quad (3.6)$$

in a more compact form

$$\sum_{l=0}^4 g_{lk} a_{lij} = f_{ij}(t_k) \quad (3.7)$$

or

$$\mathbf{G}\mathbf{a} = \mathbf{b} \quad (3.8)$$

where t_k^l was denoted by g_{lk} and $a_{li} - a_{lj}$ by a_{lij} . \mathbf{G} is referred as design matrix [14].

It may be observed that the Eq.3.5 are not linearly independent. The actual number of independent coefficients needed to be determined are only 75 out of 80. Therefore, \mathbf{G} is a singular matrix. Secondly, the number of equations are larger than the number of coefficients to be determined which made it an over determined system. In such cases, the singular value decomposition (SVD) algorithm is known to be very effective to provide least squares solution with reliable results and the same was used in the present analysis [14]. In SVD, the matrix \mathbf{G} was decomposed as,

$$\mathbf{G} = \mathbf{U}\mathbf{\Sigma}\mathbf{V}^T \quad (3.9)$$

where \mathbf{U} and \mathbf{V} were orthogonal matrices and $\mathbf{\Sigma} = \text{diag}(\sigma_1, \sigma_2, \dots, \sigma_n)$ was a diagonal matrix. The σ 's were the singular values. The polynomial coefficient vector \mathbf{a} was obtained by using the inversion of the matrix \mathbf{G} and vector \mathbf{b} ,

$$\mathbf{G}^{-1}\mathbf{b} = (\mathbf{V}\mathbf{\Sigma}^{-1}\mathbf{U}^T)\mathbf{b} \quad (3.10)$$

The matrix \mathbf{G} might be obtained by using known t_k values and the vector \mathbf{b} by using the natural logarithm of the ratios of the observed rates. It is important to note here that if $t_k \gg 1$, then the higher order terms in Eq. 3.5 might become large and one would not have converged to a solution. Therefore, irrespective of the actual values of t_k , the data were normalized by setting the highest value of t_k to 1 in the considered range of data.

4. Implementation

As discussed below, the SVD technique described in Sec.3 was employed to model the efficiency variation of the 16 modules for the period of 1 January 2006 to 31 December 2006. Considering there were discontinuities in the module rates, the whole year data had to be carefully divided into 9 segments to perform the SVD technique as described above. In each segment, only those modules were used which had recorded data continuously during the entire length of the segment. It may be noted that a module with few intermittent discontinuities in data recording was accepted as such issues could be ignored during the fit without significantly affecting the outcome. The segments were selected with 10 days overlap with the previous and the next segment to allow normalization of data as discussed later. The 9 segments selected were day number 1 – 100 (100 days), 91 – 150 (60 days), 141 – 181 (41 days), 172 – 204 (33 days), 195 – 233 (39 days), 224 – 267 (44 days), 258 – 286 (29 days), 278 – 314 (37 days), 305 – 365 (61 days). All 16 modules were used in first 4 segments, and in the 9th segment. However, due to various problems, the number of modules from 5th to 8th segments were less than 16. In 5th, 6th, 7th, and 8th segments, the number of modules were 15, 14, 3 and 14, respectively. Following the procedure as discussed earlier, the least squares fit using SVD was performed in two iterations for each segment. The data points with large deviations from the fit were excluded at the time of second iteration. This significantly improved the results in a few cases.

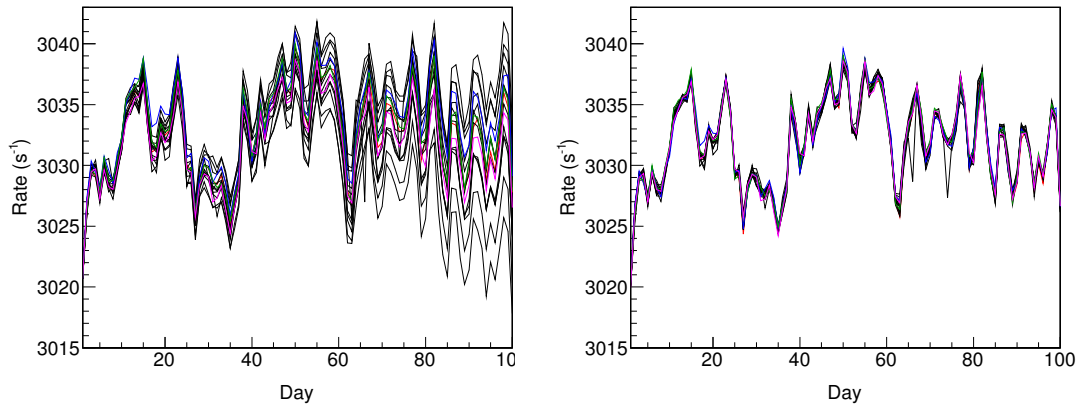


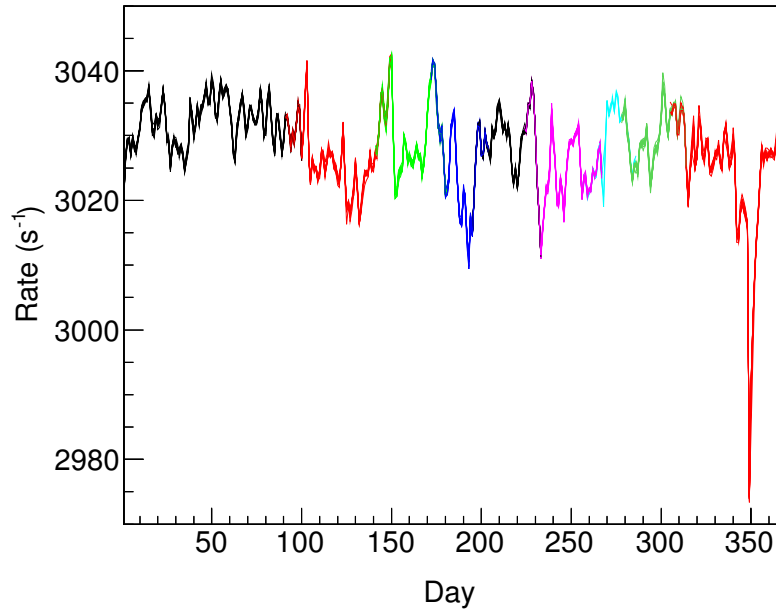
Figure 2: Daily mean muon rates of 16 modules for 1 Jan – 10 Apr 2006 before efficiency correction (left plot), after efficiency correction (right plot).

The procedure of using the SVD technique for the first segment (1 January to 30 April 2006) is illustrated below. Total 120 independent ratios with combination of 16 modules were formed for the 100 days for daily mean rates to determine 75 coefficients that represented the efficiency variation of the 16 modules. The \mathbf{G} matrix contained 120×100 rows and 75 columns. The fit coefficients obtained from the SVD are listed in Table 1. It is clearly seen that each of these coefficients is $\ll 1$, supporting the validity of the original assumption used in Eq. 3.4.

The daily mean rates were recalculated after correcting the efficiency of each 4 min rates. Fig.2 shows a comparison before and after the correction. The rates of 16 modules have been normalized to a common value at day 1 (left panel plot in Fig. 2). The near merger of 16 plots after the correction clearly demonstrated the effectiveness of the correction process.

Table 1: Coefficients obtained from the least square fit using SVD

module	a_0	a_1	a_2	a_3	a_4
1	7.1E-03	1.3E-04	2.8E-03	-6.1E-03	3.5E-03
2	3.5E-03	-8.1E-04	7.5E-04	-7.3E-04	-1.7E-04
3	3.6E-03	9.3E-04	-7.2E-03	9.3E-03	-4.9E-03
4	8.4E-03	-3.5E-03	9.0E-03	-1.4E-02	5.6E-03
5	1.0E-02	-3.3E-03	1.4E-02	-2.0E-02	1.0E-02
6	5.2E-03	1.2E-03	-8.6E-03	1.5E-02	-8.1E-03
7	5.9E-03	-1.7E-03	5.5E-03	-9.3E-03	4.7E-03
8	-7.9E-03	-2.1E-03	-8.5E-04	4.2E-03	-3.5E-03
9	-5.7E-02	3.0E-03	-1.3E-03	-1.6E-03	1.7E-03
10	-4.3E-03	1.6E-03	-9.3E-04	1.8E-04	8.7E-04
11	6.1E-03	9.9E-05	8.1E-03	-1.6E-02	9.5E-03
12	-1.9E-02	1.1E-03	-2.2E-03	4.0E-03	-1.8E-03
13	9.2E-03	4.2E-04	-3.8E-03	9.3E-03	-5.7E-03
14	2.3E-02	5.5E-03	-2.5E-02	3.9E-02	-1.9E-02
15	2.1E-02	6.9E-04	-3.0E-03	5.0E-03	-2.5E-03
16	-1.5E-02	-3.2E-03	1.3E-02	-1.9E-02	8.7E-03

**Figure 3:** Efficiency corrected rates for the 16 modules for 9 segments covering entire 2006. The big drop in the rate corresponds to a large Forbush decrease event on 14 December.

For each segment, the SVD method discussed in Sec.3 was used the 4th order polynomial coefficients that determines the efficiency variation for each module. The corrected daily mean rates of 16 modules for the 9 segments are shown in Fig. 3 and each segment is shown in different

color. It may be seen that the differences in the rates for the 16 modules in a given segment are negligible. It may also be noted that up to 4th segment, a smooth merger is seen during the 10 d overlap region without requiring any scaling of rates. Although, this outcome was not surprising, but it demonstrated the reliability of the fit, specially since the fits were independently performed. From the 5th to 9th segment, where the number of modules were less than 16, it became necessary to scale the rates to match the values in the overlap region. The scaling factors used for 5th, 6th, 7th, 8th, and 9th segments were 0.99908, 1.00082, 0.99210, 0.99892, and 0.99825, respectively. The large drop in the rate observed on 14 December 2006 was due to a Forbush decrease event occurring at that time.

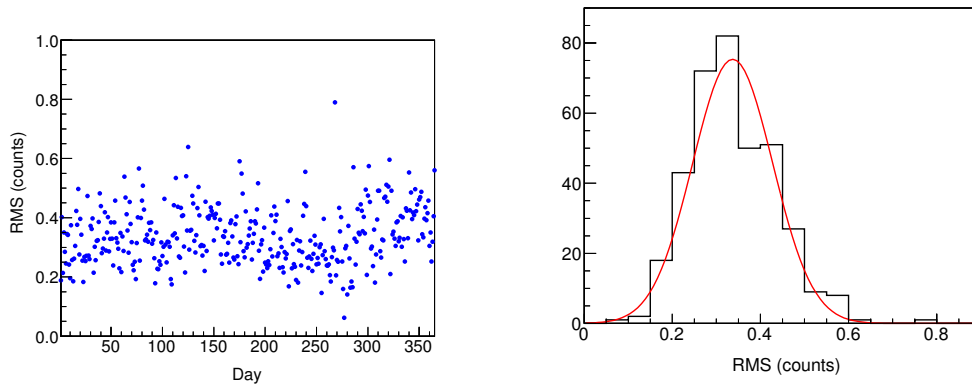


Figure 4: Plot in left shows RMS variation of efficiency corrected daily rates of the 16 modules for whole 2016 and the plot in right shows the distribution of the RMS for whole 2016.

The root mean square (RMS) spread of the efficiency corrected mean rates from 16 modules were calculated for each day for whole 2006. Out of 365 days, higher RMS values were observed for only 10 days due to fluctuations in the muon rates in some modules mainly due to noisy behaviour of the PRCs. These modules were not used and the RMS values were recalculated. The RMS variation is Fig.4. A Gaussian fit to this distribution yielded a mean value of 0.337 counts. The statistical error was 0.264 counts. The closeness of these two values shows that the irreducible systematic errors were smaller than 0.26 out of a mean muon rate of about 3000 counts. This shows a relative efficiency of 99.99% was achieved by the correction method.

5. Summary

The paper described a technique which was developed to model and correct the gradual variation of the GRAPES-3 muon telescope module rates arising due to the minute leak of PRCs using a combination of 4th order polynomial and singular value decomposition. Due to the 16 modules, it was possible to form 120 independent ratio of fourth order polynomials with a total of 80 coefficients that described the time dependent variation of the efficiency of each module. After the corrections, the RMS of the daily muon rates of the 16 modules over the year was found to be 0.34 counts which was comparable to the estimated statistical error of 0.26 count. Thus, we concluded that the efficiency correction was effective. An error of 0.34 counts in a rate of 3000 counts implies an unprecedented precision of 0.01% in the measurement of efficiency. The unique construction

of our muon detector in form of 16 modules provided sufficient redundancy to obtain such a high precision in efficiency and an unbroken record of muon intensity over the entire year. This is a very valuable data set to probe several solar phenomena. The technique has been employed for the other years of data.

Acknowledgement

We thank D.B. Arjunan, G.P. Francis, V. Jeyakumar, S. Kingston, K. Manjunath, S. Murugapandian, S. Pandurangan, B. Rajesh, K. Ramadass, V. Santoshkumar, M.S. Shareef, C. Shobana, R. Sureshkumar and other colleagues for their help in running and maintenance of the GRAPES-3 experiment.

References

- [1] S. K. Gupta et al., Nucl. Instrum. Meth. A **540** (2005) 311.
- [2] Y. Hayashi et al., Nucl. Instrum. Meth. A **545** (2005) 643.
- [3] H. Tanaka et al. J. Phys. G: Nucl. Part. Phys. **39** (2012) 025201.
- [4] A. Oshima et al., "Proc. 30th ICRC, Mexico, Vol. 2 (OG part 1), (2007), 819 – 822.
- [5] T. Nonaka et al., Phys. Rev. D **74** (2006) 052003.
- [6] K. P. Arunbabu et al., Astron. Astrophys., **555** (2013) A139.
- [7] P. K. Mohanty et al., Pramana - J. Phys. **81** (2013) 343.
- [8] K. P. Arunbabu et al., Astron. Astrophys. **580** (2015) A41.
- [9] H. Kojima et al., Astroparticle Phys. **62** (2015) 21.
- [10] H. Kojima et al., PRD **62** (2015) 121303(R).
- [11] P.K. Mohanty et al., PRL 117 (2016) 171101.
- [12] P. K. Mohanty, Ph.D. Thesis, TIFR (2014).
- [13] P.K. Mohanty et al., Astropart. Phys., **79** (2016) 2330.
- [14] H. M. Antia, Numerical Methods for Scientists and Engineers, Hindustan Book Agency, New Delhi (India) (2002).